EJSIT
European Journal of Science, Innovation and Technology
ISSN: 2786-4936
www.ejsit-journal.com
Volume 5 | Number 2 | 2025

Upward Initiated Lightning Interactions with Wind Turbines using the Extended Vertical Tri-Pole Cloud Charge Distribution Model

Godson I. Ikhazuangbe[1], Osawaru N. Osarimwian[2], F.O. Phillip-Kpae[3], Wocha Chikagbum[4], Gibson B. Iware[5]
[1]Department of Electrical and Electronic Engineering,
The University of Nottingham, United Kingdom
[2]Institute for Energy Studies, Department of Energy Engineering,
University of North Dakota, USA
[3]Department of Electrical and Electronic Engineering,
Rives State University Port Harcourt, Nigeria
[4]Department of Urban and Regional Planning, School of Environmental Sciences,
Ken Saro-Wiwa Polytechnic, Bori, Nigeria
[5]Department of Electrical/Electronic Engineering,
Ken Saro-Wiwa Polytechnic, Bori, Nigeria

ABSTRACT

Lightning can either be downward initiated or upward initiated. In the presence of a thundercloud, tall wind turbines are increasingly subjected to upward lightning attachment triggered by the wind turbine itself. Lightning strike frequency, point of lightning attachment and lightning protection systems have been evaluated based on downward initiated lightning. However, these might not be effective for upward lightning. Research has shown that the maximum electric field strength distributed on the surface of the wind turbine and the surrounding air is very important in determining the point of inception of upward leader and would help in improving lightning protection systems. In contrast to static objects, maximum electric field strength required for the inception of upward leader from wind turbine changes majorly due to blade rotation and certain blade conditions such as polluted blade surface, varying receptor sizes, receptor positions on the wind turbine, types and shapes of protection methods. Maximum electric field variations due to these blade conditions have not been considered well in literature. Analysing the maximum electric field strength and conducting experimental tests on a full-scale wind turbine is presently very difficult due to height constraint and lack of suitable equipment. This paper extends the vertical tri-pole cloud charge distribution model for analysing lightning interactions with modern large wind turbines. The model is designed and analysed in Comsol Multiphysics software and then evaluated with high voltage strike attachment test experiment. The model is intended for testing various receptor sizes, discrete receptor positions, various lightning protection systems, effect of polluted blade surface, full scale blade length as well as scaled blade tip. The blade is rotated and tested in selected five positions to investigate the performance of wind turbine lightning protection systems to determine the complete successes and failures. The proposed model has shown lightning discharges initiated from the blade surface as well as the receptor, in this case, proficiency and failure of receptor are determined. The simulation results are in agreement with that of the experiment and can be extended for larger wind turbines and also for future work. The model is suggested as a replacement for the invalidated EGM in IEC 61400 standard. Manufacturers may look at the findings of this work when dealing with the design aspects of very large future wind turbine.

Keywords: Wind Turbine, Lightning Protection, FEM, Renewable Energy

INTRODUCTION

Modern wind turbines are increasing in size due to higher megawatt, reaching height of about 220 m with blade as long as 80 m moving with a tip velocity of 60-80 m/s. They are sometimes located offshore for better wind condition, bringing them closer to lightning, and the blade is mostly affected when hit. When lightning attaches to the blade surface instead of the air-terminal, the blade and sometimes the entire wind turbine may be destroyed resulting in downtimes, loss of wind turbine, expensive cost of repair, and can cause some power companies to shut down and dismantle. Damage incidences has been recorded as well as increased insurance claims. In the past decades, lightning protection issues were well addressed for static objects and Lightning Protection Systems (LPS) are usually installed on wind turbines by applying the Electro Geometric Model (EGM) methods. The EGM relates the striking distance to the prospective peak stroke current. Recently, these methods are invalidated and according to IEC 61400-24 standards, the EGMs are no longer appropriate for large wind turbine blades.

Lightning can either be downward initiated or upward initiated. In the presence of a thundercloud, tall wind turbines are increasingly subjected to upward lightning attachment triggered by the wind turbine itself (Wang et al., 2008; Rachidi et al., 2008; Montanyà, Van Der Velde, & Williams, 2014). Report shows that upward lightning flashes are initiated from the enhancement of the electric field produced by thundercloud charge or close lightning discharges (Wang et al., 2008; Zhou et al., 2012). The critical ambient electric field also known as the stabilization electric field for the initiation of upward leaders from wind turbines produced during thunderstorms consists of two main components; (a) the static or the slow increasing component E_{cloud} due to the charging process of thunderclouds and (b) The fast-electric field charge component $\boldsymbol{\Delta}E_{\text{cloud}}$. Upward leaders in self-initiated upward lightning (Warner, Lang, & Lyons, 2014) are majorly influenced by the static or the slowly increasing electric field component E_{cloud}, with a rise rate lower than 1 kV/m/s (Cooray, 2010), i.e., during the inception of upward leaders, E_{cloud} is considered to be constant because this process has a duration of around few hundred microseconds. However, the maximum electric field strength required for the initiation of upward leaders from wind turbines is highly dependent on the blade condition and upward leader models are still being investigated. For upward propagating lightning from wind turbine, as mentioned above, the electric field in the air is near uniform being produced by the cloud and not by a stepped leader. Therefore, for upward leader formation, the strong influence of the stepped leader position is eliminated, and the formation will be dominated by the wind turbine geometry and the electric field distribution.

Lightning strike frequency, point of lightning attachment and lightning protection systems has been evaluated based on downward initiated lightning. However, these might not be effective for upward lightning. Research has shown that the maximum electric field strength distributed on the surface of the wind turbine and the surrounding air is very important in determining the point of inception of upward leader and would help in improving lightning protection systems. In contrast to static objects, maximum electric field strength required for the inception of upward leader from wind turbine changes majorly due to blade rotation and certain blade conditions such as; polluted blade surface, varying receptor sizes, receptor positions and type of protection method.

Maximum electric field variations due to these blade conditions has not been considered in literature. Analysing the maximum electric field strength and conducting experimental test on full scale wind turbine is presently very difficult due to height constraint and lack of suitable equipment. As power demand and size of wind turbine is in the increase, investigating the variations in maximum electric field strength required for the inception of upward leader from wind turbine due to varying blade conditions has become inevitable. This

paper presents the extended vertical tri-pole cloud charge distribution model for analysing lightning interactions with modern large wind turbines. The extended vertical tri-pole cloud charge distribution model made from two positive charges and a negative charge representing the idealized gross charge structure of a thundercloud is used to create an ambient field representing uniform electric field due to cloud charge distribution at 200 m above ground. The numerical model is developed with finite element analysis; COMSOL Multiphysics. The extended model is applied to a 3D electrostatics model of a full-scale wind turbine; Vestas V100 with 2 MW rated power, 164 m rotor diameter and 49 m long blade. As the blade is rotated, the variations in maximum electric field strength required for the initiation of upward leader is obtained. The model is simulated and then evaluated with high voltage strike attachment test experiment. The model is then tested on; various receptor sizes, discrete receptor position on the wind turbine, various lightning protection systems, effect of polluted blade surface, full scale blade length as well as scaled blade tip.

This work forms a platform for further investigation on modern wind turbines with regard to protecting long blades from lightning.

THUNDERCLOUD AND FIELDS INTERACTIONS WITH WIND TURBINES

This study utilizes the vertical tri-pole cloud charge distribution model made from two positive charges and a negative charge representing the idealized gross charge structure of a thundercloud. Even though the vertical tri-pole is usually used to replicate the electric fields found under a thundercloud, this model is further extended to investigate the maximum electric field strength required for the initiation of upward leaders from wind turbines due to varying blade conditions.

Initially, it is used to create an ambient field representing uniform electric field due to cloud charge distribution at 200 m above ground. By applying the extended model to a 3D electrostatics model of full-scale wind turbines; Vestas V100 with 2 MW rated power, 100 m rotor diameter and 49 m long blade, the maximum electric field strength is obtained. The peak current I_{peak} is chosen as 30 kA because it represents the general situation of lightning strikes (Ancona & McVeigh, 2001).

Thundercloud

A thundercloud is a cumulus cloud with a towering or spreading top, usually charged with electricity and capable of producing lightning and thunder. It may also be defined as a lightning-producing cumulonimbus. This definition is due to the fact that the cloud type termed cumulonimbus is the primary source of lightning and it is commonly referred to as the thundercloud. Though, not every cumulonimbus will produce a lightning (Imyanitov, Chubarina, & Shvarts, 2009). Thunderclouds are complex, large and short-lived. A system of thunderclouds is referred to as thunderstorm. Thunderstorms have been observed and investigated, Rodrigues et al. (2009), analysed thunderstorm activity in Portugal.

Gross Charge Distribution in a Thundercloud

Basically, as generally accepted, the features of the cloud charge structure consist of, (a) A net positive charge near the top, (b) A net negative charge bellow it, and (c) An additional positive charge at the cloud bottom. It should be noted that positive and negative charge coexist in any region of the cloud, irrespective of the polarity of the net charge in the region (MacGorman & Rust, 1998).

The Thunder Cloud Model

The charge structure in a thundercloud is usually replicated by three vertical stacked point charges or spherically symmetrical charge volumes. It consists of a vertical tri-pole

made from a negative charge and two positive charges. A summary of various cloud models have been listed in (Rakov & Uman, 2003; Bazelyan & Raizer, 2000). The cloud model that has been implemented and simulated in this work is taken from (Rakov & Uman, 2003; Bazelyan & Raizer, 2000; Cooray, 2010). The model is illustrated in Figure 1, it has positive charge at the top, negative in the middle, and a smaller positive at the bottom, and the ground modelled as a perfect conductor. The top two charges are also called the main charges and are usually specified to be equal in magnitude. Sometimes, the lower positive charge is not present. The top two charges form a dipole, said to be positive because the positive charge is above the negative charge, this gives an upward-directed dipole moment.

In the simulation, the three charges of +40C, -40C and 3C are placed at height of 12, 7 and 2 km from the ground respectively and modelled as spheres of radii 900m for the 40C charges and 150 m for the charge of 3C (Rakov & Uman, 2003; Peesapati & Cotton, 2009). The size of the spheres is such that during meshing, the accuracy of the electric field in the area of interest within the model is ensured.

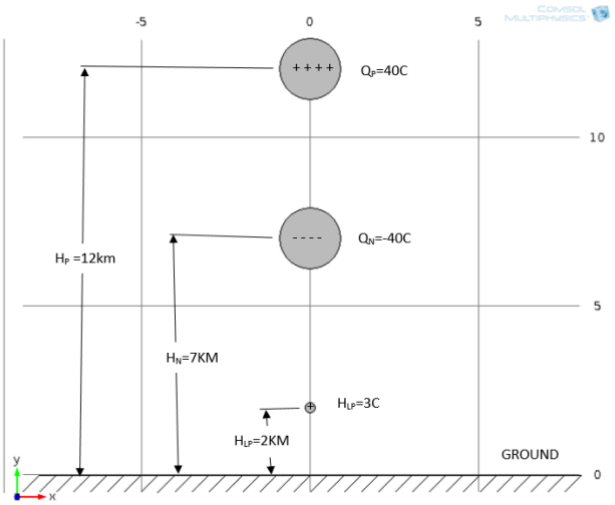

Figure 1: A vertical tri-pole made from two positive charges and a negative charge representing the idealized gross charge structure of a thundercloud

Note: Q_p is the main positive charge, Q_N is the main negative charge, H_{LP} is the lower positive charge and H_P, H_N and H_{LP} are their various distances (in kilometre) from ground.

Electric Field Intensity

The electric field intensity (**E**) due to the system of three charges (Qp, Q_N and H_{LP}) shown in Figure 1 is found by replacing the ground (perfectly conducting ground) with three image charges and by using the principle of superposition, the total electric field being the vectorial sum of six (three from the actual charges and three from their images) contributions.

Computation of Electric Field on Ground Surface

Figure 2 shows the computation of the electric field (equation 1) on the ground surface owing to the main negative charge (Q_N) and its image. The actual charge's magnitude and that of its image are equal, and the contribution of each is found as in (Sadiku, 2014).

$$|\mathbf{E}^{(-1)}| = |\mathbf{E}^{(+1)}| = \frac{|Q|}{4\pi\varepsilon_0(H^2+r^2)} \quad (1)$$

Figure 2 shows the method of images used for finding the electric field due to a negative point charge (Q_N) above ground (a perfectly conducting ground) at a field point located on the ground surface.

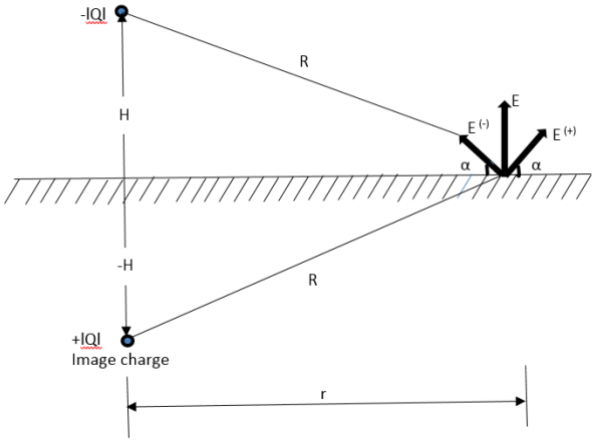

Figure 2: The method of images

From the method of image, it is apparent that, as expected from the boundary condition on the surface of a perfect conductor, the components of the electric field (equation 2), that is tangential to the ground plane due to the actual negative charge and its image cancel each other. The electric field components that is normal to the ground plane add, and the total normal field magnitude is twice the contribution from either the actual negative charge or its image:

$$|\mathbf{E}| = 2|\mathbf{E}^{(-1)}|\cos(90^0 - \propto) = 2|\mathbf{E}^{(+1)}|\cos(90^0 - \propto) = 2|\mathbf{E}^{(-1)}|\sin \propto = \frac{|Q|H}{2\pi\varepsilon_0(H^2+r^2)^{3/2}} \quad (2)$$

For the variation in |**E**| as a function of H and r with I**QI** = constant. Rewriting Eq. 2:

$$|\mathbf{E}| = \mathbf{k}\frac{\sin\propto}{R^2} \quad (3)$$

Where $\mathbf{k} = \frac{|Q|}{2\pi\varepsilon_0}$ **and** $\mathbf{R^2} = (H^2 + r^2)$.

Therefore, for two vertically stacked charges of equal magnitude, i.e., the main positive charge (Qp) and main negative (Q_N) charge (Figure 1), each of these two charge's relative contributions to **E** depends on r. The lower charge dominates the electric field at r = 0 because it is closer and sine α is the same for both charges. But the relative contribution from the upper charge increases just as r increases. The contribution from the upper charge becomes dominant at a certain distance and the total electric field i.e., the sum of the contributions due to the two charges, changes its polarity. This distance is referred to as the reversal distance. For two vertically stacked charges of opposite polarity but equal magnitude the reversal distance, D_0, is given by

$$\mathbf{D_0} = [(H_P H_N)^{2/3}(H_P^{2/3} + H_N^{2/3})]^{1/2} \quad (4)$$

H_p is the heights of the positive charge and H_N is the heights of the negative charge. Therefore, for a positive dipole, it is expected that at far ranges the total electric field is positive, while at near ranges it is negative.

Theory for Electric Field Interface

COMSOL Multiphysics contains physics interfaces for the modelling of static electric fields and currents. It is a computer simulation program that accommodate the physics of lightning interactions with grounded objects and can be used to evaluate protection procedures.

Charge Relaxation Theory.

The different physics interfaces can be interpreted in terms of the charge relaxation process. The fundamental equations involved are Ohm's law ($J = \sigma E$) the *equation of continuity* (equation 5).

$$\frac{\partial \rho}{\partial t} + \nabla . \mathbf{J} = \mathbf{0} \tag{5}$$

and Gauss' law (equation 6)

$$\nabla . (\boldsymbol{\varepsilon} \mathbf{E}) = \boldsymbol{\rho} \tag{6}$$

By combining these, the following differential equation can be deduced for the space charge density in a homogeneous medium

$$\frac{\partial \rho}{\partial t} + \frac{\sigma}{\varepsilon \rho} = \mathbf{0} \tag{7}$$

The solution to 7 is given as

$$\mathbf{P}\,(\mathbf{t}) = \boldsymbol{\rho}_{\mathbf{0}} \mathbf{e}\text{^}(-\mathbf{t}/\boldsymbol{\tau}) \tag{8}$$

Where $\boldsymbol{\tau} = \boldsymbol{\epsilon}/\boldsymbol{\sigma}$, and $\boldsymbol{\tau}$ is called the charge relaxation time. For a good conductor, such as copper, τ is of the order of 10^{-19}s but for a good insulator such as silica glass, it is of the order of 10^{3}s. It becomes infinite for a pure insulator.

Electrostatics Interface

The electric potential V for static conditions, is defined by the relationship;

$$\boldsymbol{E} = -\boldsymbol{\nabla} \mathrm{V} \tag{9}$$

With equation (5) combined with the constitutive relationship $\boldsymbol{D} = \varepsilon_0 \mathbf{E} + \mathbf{P}$ between the electric displacement **D** and the electric field **E**, it is possible to represent Gauss' law as the following equation:

$$-\nabla . (\varepsilon_0 \nabla \mathrm{V} - \mathbf{P}) = \boldsymbol{\rho} \tag{10}$$

In the above equation, the physical constant, ε_0 (SI unit: F/m) is the permittivity of vacuum, ρ (SI unit: C/m^3) is space charge density and P (SI unit: C/m^2) is the electric polarization vector. The electrostatic field in dielectric materials is described by this equation.

For in-plane 2D modelling, the electrostatics interface adopts a symmetry where the electric potential varies in the x and y directions only and is constant in the z direction. This suggests that the electric field, **E**, is tangential to the xy-plane. Due to this symmetry, the same equation is also solved in the 3D case. The interface evaluates the following equation where d is the thickness in the z direction:

$$-\nabla . \mathbf{d}(\varepsilon_0 \nabla \mathbf{P} - \mathbf{P}) = \boldsymbol{\rho} \tag{11}$$

The axisymmetric type of the interface considers the situation in which the fields and geometry are axially symmetric. For this case the electric potential, V is constant in the φ direction, which infers that the electric field is tangential to the rz-plane.

Let E_2 be the final electric field value after the charge removal due to lightning, and E_1 be the initial electric field value from original cloud charge distribution. Therefore, an electric field change is found as the difference between E_2 and E_1. The corresponding electrostatics field change for any charge removed from the cloud, is the negative of that charge contribution to the initial electric field. Assuming negative cloud charge's complete neutralization due to cloud-to-ground discharge, the resultant net electric field change at any distance will be negative, this is because the upward-directed positive electric field due to the negative charge (Figure 2) becomes zero. Polarity reversal will be exhibited by the resultant net field change as a function of distance if both main negative and main positive charges are neutralized via an intra-cloud discharge. It should be noted that the positive field values are significantly smaller than the negative field values. The occurrence of the polarity reversal is because the net field change to the total electric field from these two charges, is the negative of the sum of the contributions, from these two charges. At close ranges, this sum is positive and negative at far ranges. Electric field changes related to upward initiated lightning was observed in Gaisberg tower (Zhou et al., 2011).

Ambient Field Representing Uniform Electric Field Due to Cloud Charge Distribution at 200 m above Ground

An increased electric field at ground level produced by the electrical charge within a thundercloud can result in the production of upward leaders from a structure before the formation of a stepped leader. The attachment point is determined by these formation points of these upward leaders.

The results of the electric field at ground from the system of three charges shown in Figure 1 agrees with the report in (Rakov & Uman, 2003), with maximum ambient field of just over 5kV/m. These values are used in this work and an upward-directed electric field is defined as positive (Rakov & Uman, 2003).

In order to analyse the maximum electric field strength required for the initiation of upward leaders from wind turbines, the information from the cloud model is combined with the wind turbine model in the simulation. As mentioned above, the vertical tri-pole model is used to create an ambient field representing a uniform electric field due to cloud charge distribution at 200 m above ground. A uniform electric field produced by a plane electrode located 200 m above the ground is then applied on the wind turbine model. The magnitude of the applied electric field is 1MV/m (200 X 5KV/m = 1000000V/m). This is based on the results found from Malan's charged cloud model (Rakov & Uman, 2003). Figure 3 shows the simulation model while Figure 4 is the meshing. The electrode's polarity is negative; the environment is modelled as air and the wind turbine is sited on the ground. The dimension of the electrode is large enough to prevent flashover from the edges.

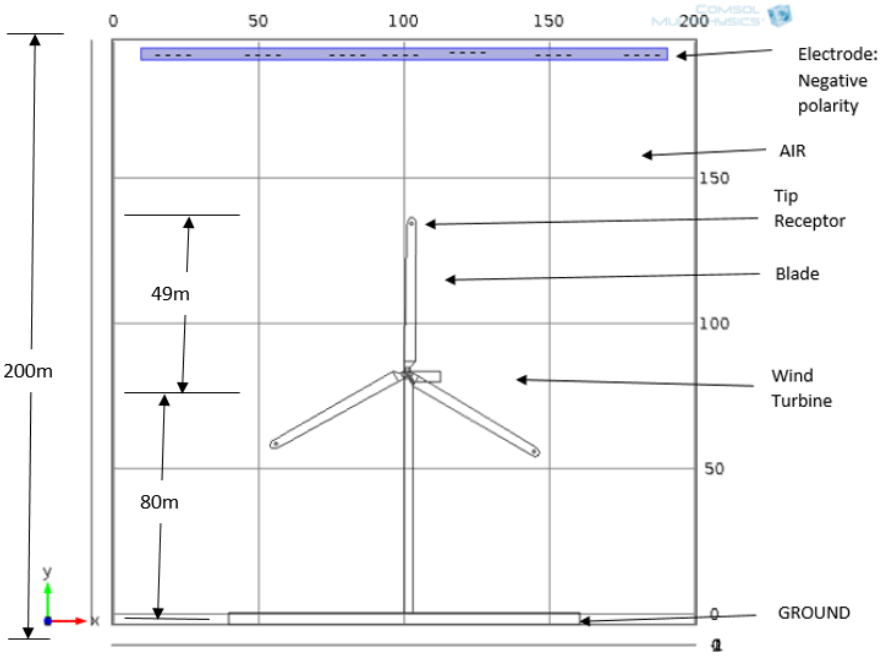

Figure 3: Simulation model

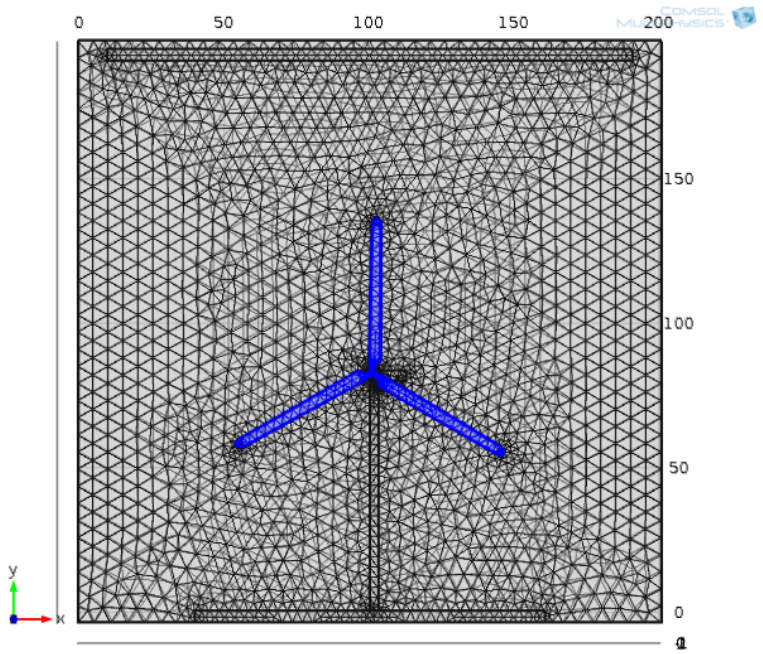

Figure 4: Model meshing

Wind Turbine Model

A modern wind turbine is used as case study in this work, Vestas V100 with 2 MW rated power, 100 m rotor diameter, swept area 7.854m^2 and 49 m long blade. V100 is a horizontal axis wind turbine with three blades. The blade is made of fibred glass with a relative permittivity: of 4.2, conductivity:1.0×10^{-14} S/m, blade thickness: 10 cm, chamber length: 0.9 m, maximum chord 3.9 m (varied at blade root and tip). The wind turbine nacelle and tower are conductive and are set to ground potential. Hub height (height from the lowest part of the tower to the Centre of the hub) is 80 m. The tower is tubular steel type. The nacelle is 10.4 m long and 3.5 m wide. V100 is shown below in Figure 5.

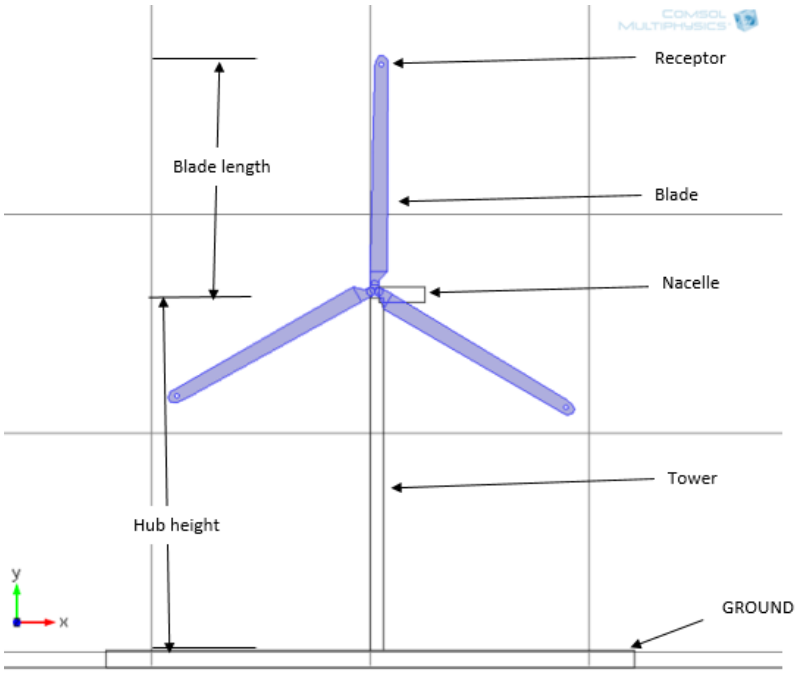

Figure 5: Wind turbine model

Full Scale Blade

A sample of a full-scale blade is shown in Figure 6.

Figure 6: V164-80m long wind turbine blade (Milelr, 2023)

Figure 7 is a full-scale blade model design.

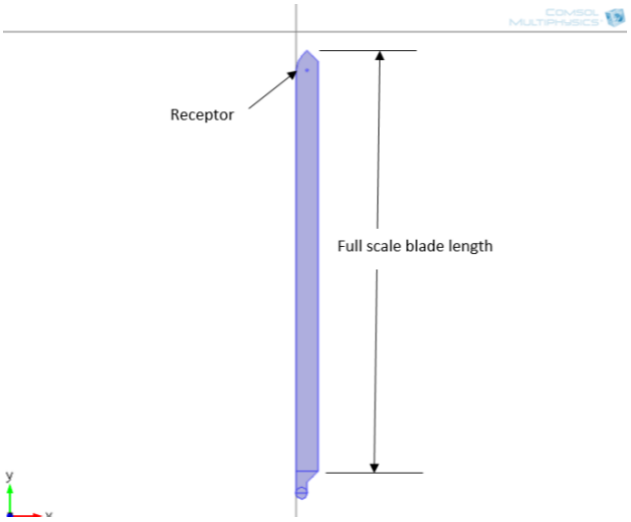

Figure 7: Full scale blade model

Lightning Protection Air-Terminal

The lightning protection system is integrated into the model design. Wind turbine lightning protection systems usually consist of an internal down conductor with air-termination systems. The type of air-terminal used in this work is the tip receptor method set at 2 m from the tip of the blade. The receptor is grounded or earthed so as to take the lightning current to ground. The receptor's design is such that it can be activated or deactivated when the need arises during analysis. It is 10 mm in diameter and made of copper (conductivity: 6.0×10^{-7}S/m). The tip receptor (purple colour) design is shown in Figure 8.

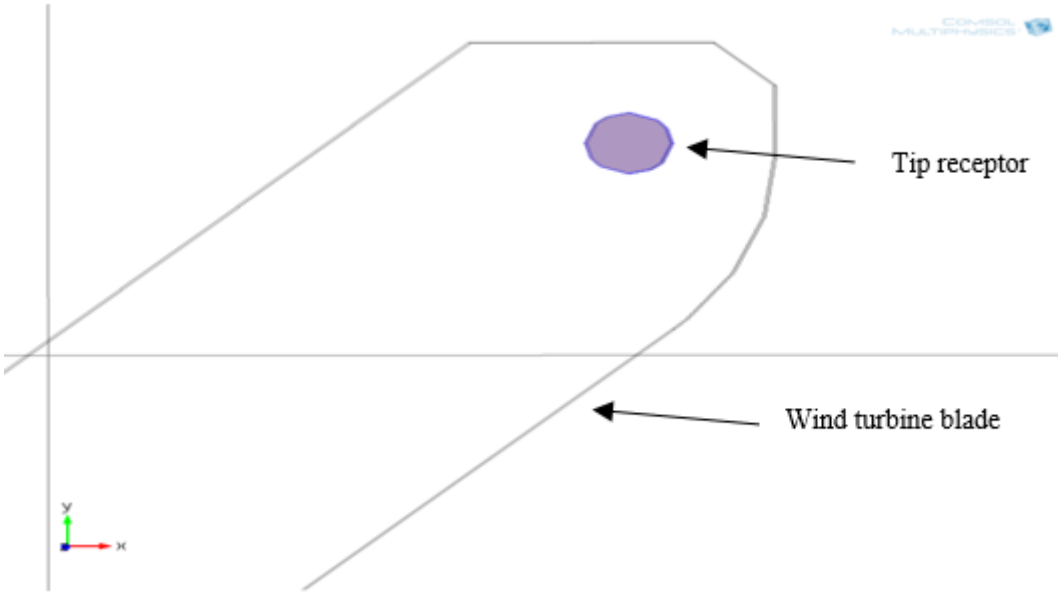

Figure 8: Tip receptor design

Material Content for the Design

The materials used for the turbine blade, air, thundercloud, the lightning protection systems and ground model's designs are shown in Tables 1, 2, 3 and 4 respectively.

Table 1: Material used for Turbine blade design

Property	Name	Value	Unit	Property Group
Relative permittivity	Epsilon	4	1	Basic
Relative permeability	Mur	1	1	Basic
Density	Rho	2200[kg/m^3]	kg/m^3	Basic
Electrical conductivity	Sigma	$1.0x10^{-14}$[s/m]	s/m	Basic
Thermal conductivity	K	1.1[w/(m*k)]	w/(m*k)	Basic
Heat capacity at constant pressure	C_p	480[J/(kg*k)]	J/(kg*k)	Basic
Refractive index	N	1.5	1	Refractive index
Refractive index, imaginary part	Ki	0	1	Refractive index
Young's modulus	E	$74X10^9$[pa]	Pa	Young's modulus and Poisson's ratio
Poisson's ratio	Nu	0.3	1	Young's modulus and Poisson's ratio

Table 2: Materials used for thunder cloud and lightning protection systems designs

Property	Name	Value	Unit	Property Group
Electrical conductivity	sigma	$5.998x10^7$[s/m]	s/m	Basic
Coefficient of thermal expansion	alpha	$17x10^6$[1/k]	1/k	Basic
Heat capacity at constant pressure	C_p	385[J/(kg*k)]	J/(kg*k)	Basic
Density	Rho	8700[kg/m^3]	kg/m^3	Basic
Thermal conductivity	K	400[w/(m*k)]	w/(m*k)	Basic
Young's modulus	E	$110X10^9$[pa]	Pa	Young's modulus and

				Poisson's ratio
Poisson's ratio	Nu	0.35	1	Young's modulus and Poisson's ratio
Reference resistivity	Rho0	1.72x108[ohm*m]	Ω*m	Linearized resistivity
Resistivity temperature coefficient	alpha	0.0039[1/k]	1/k	Linearized resistivity
Reference temperature	Tref	298[k]	K	Linearized resistivity

Table 3: Materials used for Air as the environment

Property	Name	Value	Unit	Property Group
Relative permittivity	epsilonr	1	1	Basic
Relative permeability	Mur	1	1	Basic
Ratio of specific heat	gamma	1.4	1	Basic
Electrical conductivity	sigma	0[s/m]	s/m	Basic
Dynamic viscosity	Mu	Eta(T[1/K])[pa*s]	Pa*s	Basic
Density	Rho	Rho(Pa[1/pa],T[1/k])[kg/m^3]	kg/m^3	Basic

Table 4: Material used for a perfectly conducting ground (an ideal ground) design

Property	Name	Value	Unit	Property Group
Relative permittivity	Epsilon	1	1	Basic
Relative permeability	Mur	1	1	Basic
Electrical conductivity	sigma	$5.998x10^{-7}$[s/m]	s/m	Basic
Coefficient of thermal expansion	alpha	$17e^{-6}$ (1/k)	(1/k)	Basic
Heat capacity at constant pressure	C_p	385[J/(kg*k)]	J/(kg*k)	Basic
Density	Rho	8700[kg/m^3]	kg/m^3	Basic
Thermal conductivity	K	400[w/(m*k)]	w/(m*k)	Basic
Young's modulus	E	$110e^{-9}$[pa]	Pa	Young's modulus and Poisson's ratio
Poisson's ratio	Nu	0.35	1	Young's modulus and Poisson's ratio
Reference resistivity	Rho0	$1.72e^{-8}$[ohm*m]	Ω*m	Linearized resistivity
Resistivity temperature coefficient	alpha	0.0039[1/k]	1/k	Linearized resistivity
Reference temperature	Tref	298[k]	k	Linearized resistivity

Procedure for Evaluation

The electric field due to thunder cloud charge can be calculated using these electrostatics equations. The governing equations are solved with FEA software and the computational domain is shown in Figure 3.

Different configurations are applied on the wind turbine to investigate the effect of blade conditions on initiation of upward leader. In each case, the evaluation is done as the blade is rotated through -60^0 and 60^0 from the vertical position. The blade in the vertical position in Figure 3 is referred to in this paper as blade A and only the results for blade A are

provided. Also, values are obtained from the blade tip, leading edge, trailing edge, the receptor tip and sometimes the blade surface. The focus is on evaluating the efficiency of the lightning protection systems by obtaining the maximum electric field strength required for the initiation of upward leader due to thunder cloud charge. The positions with higher electric field strength are considered to have higher possibility of inception of upward leader. Results are plotted and compared for values obtained from the blade tip, leading edge, trailing edge and the receptor tip. The most efficient situation in this analysis is the one with highest electric field on the receptor and minimum at the tip, leading edge, trailing edge and the entire blade surface.

In order to investigate the effect of blade conditions on the electric field strength, the simulation is first conducted on the wind turbine without the receptor and then the receptors is used as the blades are rotated.

Unprotected Wind Turbine

Figure 9 shows an unprotected wind turbine model under the influence of thunder cloud electric field. The receptor is disabled; leaders can incept from any part of an unprotected wind turbine with a consequence of lightning damage.

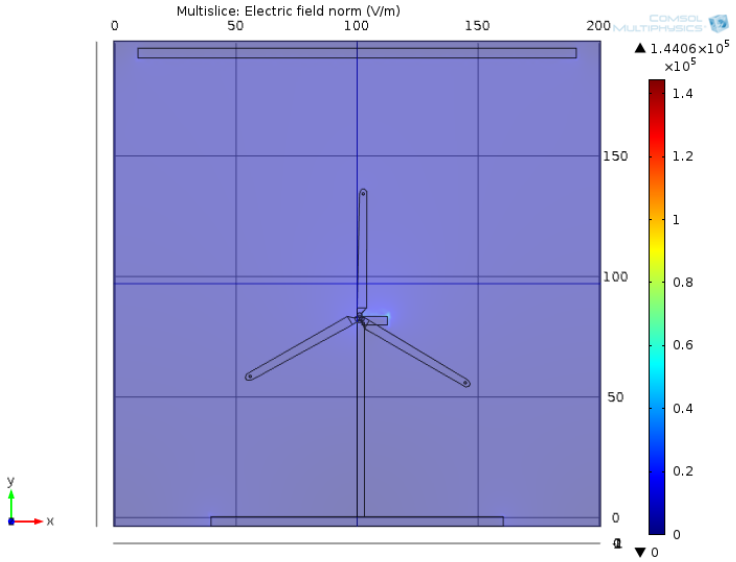

Figure 9: Unprotected wind turbine

Protected Wind Turbine

A protected wind turbine model is shown Figure 10 below; the receptor is enabled. When the wind turbine is put in the electric field, field enhancement is observed at certain positions as shown. The level of electric field intensification is predominantly high around the lightning protection system of the wind turbine model and at the blade tip. This intensification will allow the formation of upward streamers. From the diagram, field enhancement is seen, it is apparent that upward leader will first incept from the blade in the vertical position. Lightning strike might initially attach to the lighting protection device depending on its ability to emit leader relative to the ability of the surrounding surface.

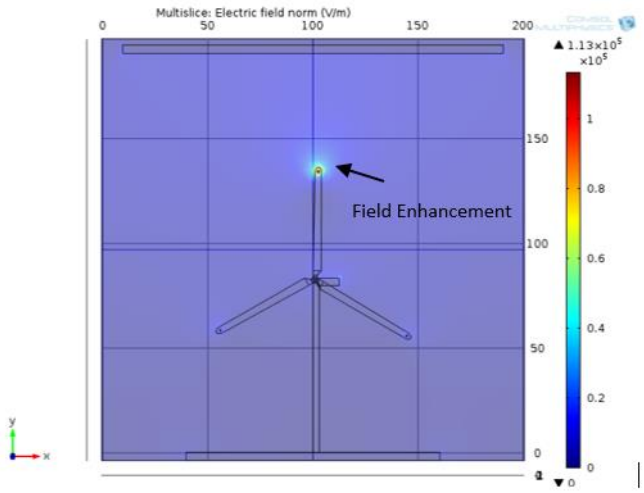

Figure 10: Protected wind turbine

As mentioned above, the simulation result shows a high probability of inception of upward streamer from the blades. The highest been the blade (blade tip and receptor) at the vertical position, then the nacelle, and also the receptor of the other two blades. Upward initiated lightning production, at first, depends on a given level of electric field enhancement existing around a component and also their position (Alonso & Irastorza, 2008). The results correlate with experimental and actual lightning data on points of leader attachment and upward leader initiation points. However, the electric field is affected by the blade conditions.

As mentioned earlier, when the wind turbine is protected, by activating the receptors, field enhancement is seen. Figure 11 shows the detailed activities around the receptor, these include; the upward positive polarity for streamer activities, the negative polarity going to ground through ground wire, positive polarity on the blade surface. Also shown is the produced corona charge (qc) which lowers the electric field on the tip inhibiting the occurrence of a streamer.

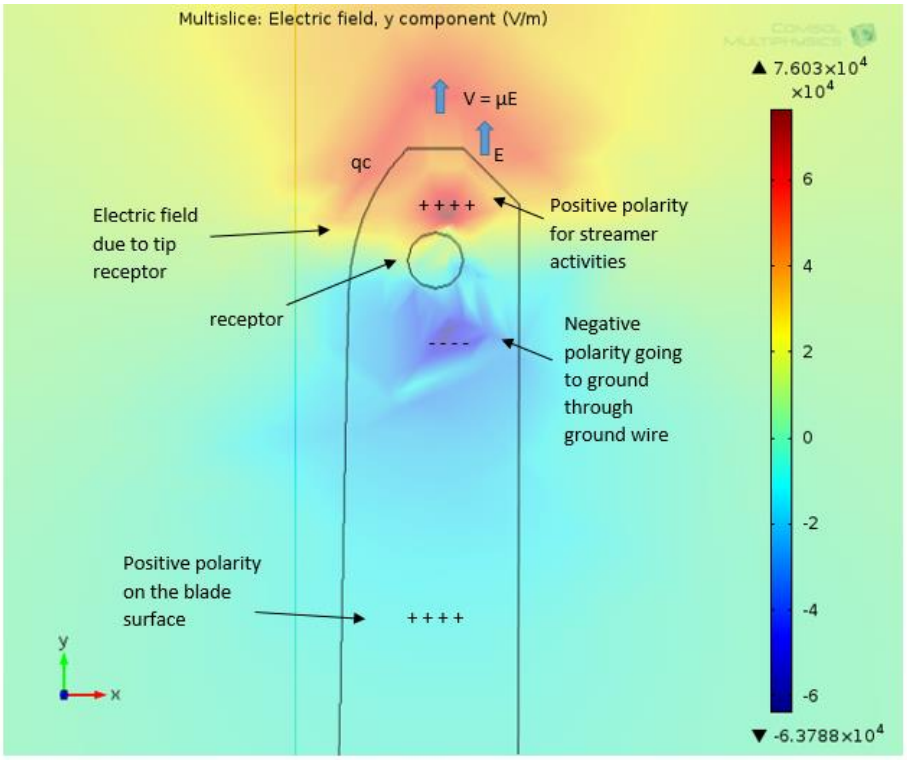

Figure 11: Activities around the receptor preceding leader initiation

APPLICATION

The extended vertical tri-pole cloud charge distribution model is applied on wind turbine considering various blade conditions. The model is tested on; various receptor sizes, discrete receptor position on the wind turbine, various lightning protection systems, effect of polluted blade surface, full scale blade length as well as scaled blade tip. These tests are conducted as the blade is rotated.

Rotated Wind Turbine

Blade A is moved counter clockwise for analyzing rotation. The evaluation is done as the blade is rotated through -60^0, -55^0, -50^0, -45^0, -40^0, -35^0, -30^0, -25^0, -20^0, -15^0, -10^0, -5^0, 0^0, 5^0, 10^0, 15^0, 20^0, 25^0, 30^0, 35^0, 40^0, 45^0, 50^0, 55^0 and 60^0 from the vertical position. The model used for rotation mode is shown in Figure 12.

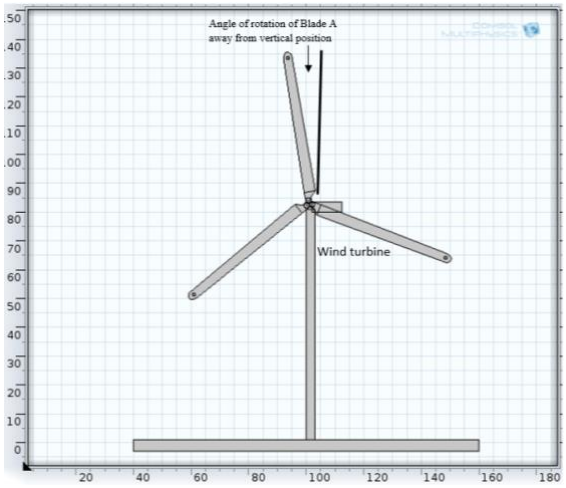

Figure 12: Rotation model

Figure 13 shows the simulation for the rotated blade. As observed, the maximum electric field strength required for the initiation of upward leader from wind turbine changes as the blade is rotated.

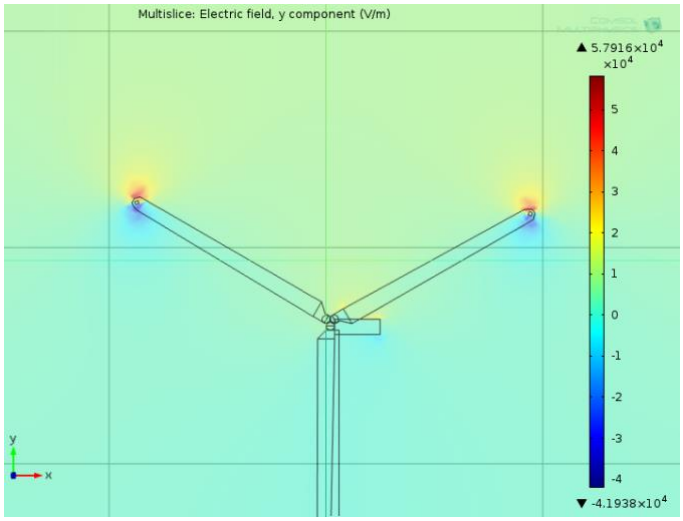

Figure 13: Rotated state

Figure 14 shows the maximum electric field distribution as blade A is rotated from -60^0 to $+60^0$ from the vertical position: (a) 30^0; (b) vertical position; (c) -30^0; (d) 60^0; and (e) -60^0. It is generally observed that the electric field strength at the tip region appears to be higher than that at the inboard region. This is corroborative of laboratory experiments and field observations indicating that the tip is more exposed than other part (Peesapati et al., 2011; Jeong-min, Sung-man, & Munno, 2024), and that upward leader is more likely to initiate from the tip receptor. When lightning attaches to the receptor, it will be conducted to ground through ground wire without causing damage to the turbine. This is the intent of the lightning protection design. If lightning is attached to the blade surface instead of the receptor, the blade and even the entire wind turbine can be destroyed. The positions with higher electric field strength are considered to have higher possibility of inception of upward leader. The negative polarity going to ground through ground wire as shown in Figure 14 is usually confined to the ground wire and not on the surface of the blade, therefore, only the positive parts of the electric field strength are relevant.

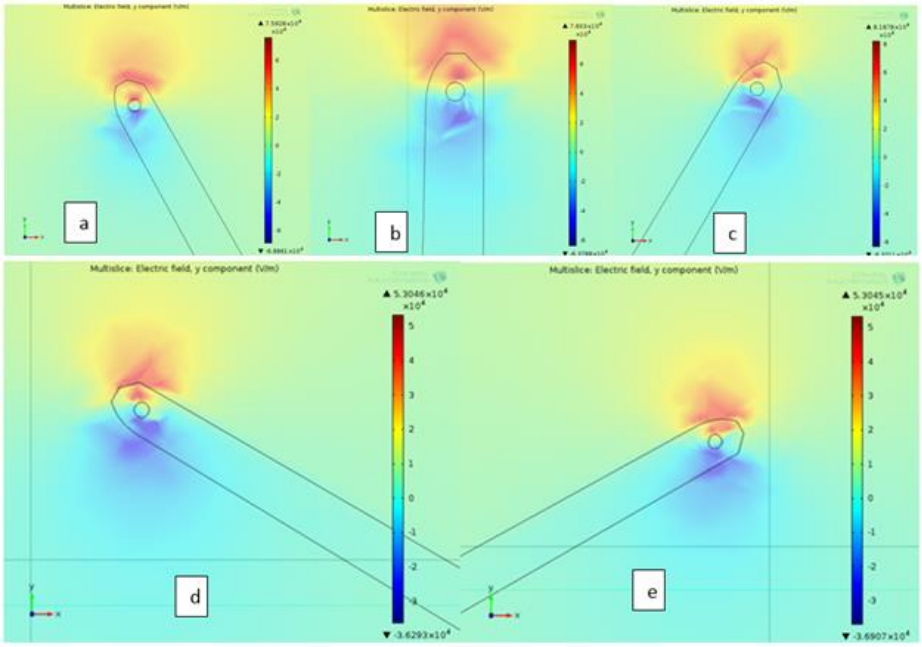

Figure 14: Maximum electric field distribution as blade A is rotated from -60 to +60 degrees from the vertical position: (a) 30; (b) vertical position; (c) -30; (d) 60; and (e) -60.

The results for different blade position are shown in Table 5 and are plotted (Figure 15).

Table 5: Maximum electric field strength distribution (kV/m)

Angle from Vertical	Blade tip	Leading edge	Trailing edge	Receptor
-60^0	20.12	36.25	0.43	60.78
-30^0	43.96	42.64	21.93	121.0
0^0	58.29	26.93	45.70	193.0
30^0	45.03	2.04	51.43	135.0
60^0	21.27	-14.83	37.41	61.35

Field strength versus blade position

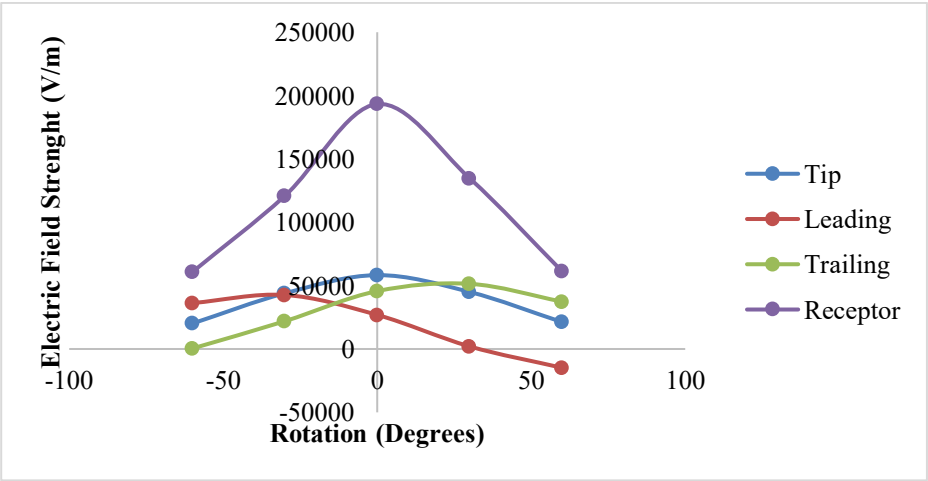

Figure 15: Maximum electric field strength distributions as blade A is rotated

The simulation result is shown in Figure 15. The electric field distribution on the blade is shown. The maximum electric field plot shows that the value at the receptor tip is highest at the vertical position, followed by the blade tip also at the vertical position, the leading edge at -60^0 and then, trailing edge at 30^0. The electric field distribution is highest at the receptor and as such, leader will incept from it first followed by other part of the blade in the sequence as depicted by the plot.

LIGHTNING DISCHARGE EXPERIMENTS

This section describes the validation of the simulation model used in evaluating the maximum electric field strength required for the initiation of upward leader from wind turbine due to varying blade conditions. High voltage test is carried out to study the development of streamers on different blade positions of a wind turbine blade made of fiberglass to validate the obtained simulation results. Obtained experimental results are compared with that of simulation and then discussed.

Experimental Setup and Procedure for High Voltage Strike Attachment Test

Lightning attachment to wind turbines has gained attention, with many research works focused on downward propagating lightning. Nevertheless, a few work, done on upward propagating lightning (Particularly due to electric fields from winter clouds developed at lower altitudes) has shown that apart from the fact that tall wind turbine can increase the number of lightning strike, due to rotation, turbines are triggering their own lightning (Wang et al., 2008; Rachidi et al., 2008; Montanyà, Van Der Velde, & Williams, 2014), indicating that large portion of the lightning that attach to a wind turbine are upward initiated. This type of lightning is majorly influenced by the slowly increasing electric field with a rise rate lower than 1 KV/m/s (Cooray, 2010), and the formation is dominated by the electric field distribution and the wind turbine geometry. The stepped leader position influence is removed. Therefore, the analysis in this work only involves upward lightning strike.

The high voltage strike attachment test is usually applied to determine specific lightning attachment points on a structure. The main idea is to know from where upward initiated leaders or answering leaders are emitted.

The test arrangement is intended to result in initiation of electrical activity, such as corona, streamers and leaders at a wind turbine blade just before a lightning strike attachment. Immediately ionization of the air at the wind turbine blade test specimen is initiated, the incepted streamer will progress towards the ground which has a large geometry and is intended to represent an electric field equipotential surface some distance from a blade extremity. In this manner, the influence of the external test electrode on test results is minimized. Figure 16 shows the setup of the test arrangement, this includes; high voltage generator, blade test specimen and ground. This test setup is chosen because it usually allows a larger dimension external electrode (i.e. a conductive surface on the floor of the laboratory) and a more realistic electric field environment during the test around the blade specimen to be provided. The test is performed by elevating the specimen above a grounded test plane in a high voltage laboratory. This grounded plane simulates an equipotential plane of the electric field between the blade tip and an approaching lightning leader of a downward initiated lightning flash or the static background electric field present prior to an upward initiated lightning flash.

There are a number of lightning protection methods used on wind turbines, these includes; Receptors, Metallic Cap, Metallic Conductor on the Blade Tip, Mesh, Ring Electrode (Zavareh, 2012) and the Backside Electrode (Minowa et al., 2012) methods, also the combined cap and receptors method recommended in (Godson et al., 2019) for offshore wind turbines. However, modern onshore wind turbines are predominantly protected with the

receptor method. More also, multiple receptors on the blade have been a focus of research but the single-receptor method has remained the preferred choice. Therefore, only the single-receptor method is considered in this experiment.

The receptor though effective (Shindo, Asakawa, & Miki, 2011), also failed in so many instances as mentioned in (Yoh & Shigeru, 2011; Yokoyama, 2011). The efficiency of the receptor is dependent on its interception proficiency which is its ability to intercept a lightning stroke. The test aims at defining efficiency of the receptor achieved by a pass or fail in their ability to influence electric field distribution and to determine to which point lightning discharge will attach on the wind turbine blade. The test environment experienced by the wind turbine blade is similar to real lightning situation and the entire blade is totally affected by the external field prior to a lightning strike (Godson et al., 2019).

The high voltage waveform used is a double exponential switching type impulse voltage with rise times in order of 50-250μs and decay times of 2000μs. This voltage waveform is selected since it is the most representative of the electric field in the vicinity of a structure during an initial leader attachment.

Test Specimen

In order to assess the normal distribution of the points of discharge attachment on the blade surface, a large sized wind turbine hit by natural lightning strike is experimentally required while it is rotating, this can only be done in the natural lightning laboratory such as in Florida (Peesapati & Cotton, 2009). The protection evaluation is done using 3 m blade tip section that is a part of Vestas V100 wind turbine, with 2 MW rated power, 100 m rotor diameter and 49 m long blade made of glass fibers reinforced polyester, cut from an actual blade. This size is adopted because most of the lightning attachments are located in the tip area of the blade. As compared to full scale wind turbine, testing with small specimens like 3 m of a full-scale length, makes it possible to perform many tests within a limited amount of time and the duration for the test in this experiment is within one week. The elevated blade specimen is connected to the output of a Marx generator injecting high voltage impulses into the lightning protection system (receptor) of the blade. Blade thickness is 10 cm, chamber length: 0.9 m, maximum chord 3.9 m. The receptor is 10 mm in diameter placed 1.5 m from the blade

The receptor is connected to ground through a down conductor of 6 mm^2 cross section area embedded in the blade. A receptor fixed in a blade tip is shown above in Figure 5.

Test Setup

The tests are performed on the test setups illustrated in Figure 16 having the blade specimen elevated above a ground plane in the high voltage laboratory.

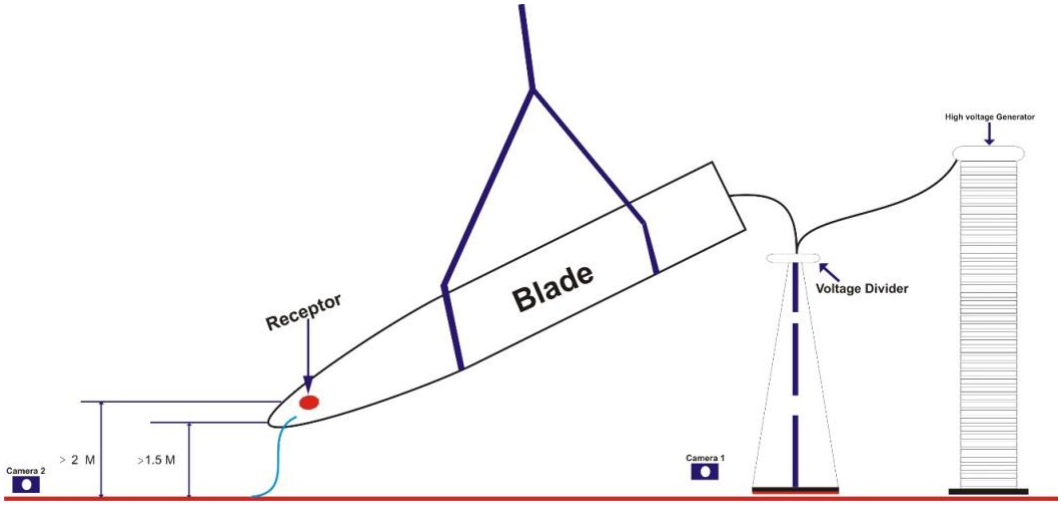

Figure 16: Initial leader attachment test setup

It includes the following:

1. The blade sample described above,
2. Marx generator with resistances and capacitances configured to generate desired voltage waveform.
3. Voltage divider and additional measuring system
4. Digital camera used to determine and show the discharge attachment point to the blade sample.

The size of the ground plane below the blade tip is large enough to avoid discharges from the blade to the edges of the ground plane.

Test Procedure

The Marx generator is adjusted to produce double exponential voltage waveforms D with positive and negative polarity. The blade is then suspended above the ground plane with all distances as shown in the figure. The output of the Max generator is connected to the down conductor inside the blade sample and the down conductor is then connected to the lightning receptor.

Five pulses are first applied to the model blade without receptor, then various configuration of blade sample and a picture is taken at each discharge. High voltage strike attachment test is performed with the test specimen blade positioned in different orientations as prescribed by IEC 61400-24. In each orientation, various blade conditions can be experimented on. Polluted blade surface was achieved with salt contamination 10 g/l solution of sodium chloride (NaCl) sprayed on the surface of the blade. The waveform for each discharge was recorded and, in each case, the peak value and the time to flashover was determined. Determination of the attachment points was made possible by capturing images of the discharge with a digital camera.

As the blade rotates, it was tested in selected five positions to investigate the performance of wind turbine lightning protection systems on initiation of upward leader. The positions of the blade are chosen to determine the complete successes and failures of receptor. These positions are shown in Figure 17 (b). They are; (b) vertical, (c) 45^0 (Trailing edge facing the cloud) (TEFC), (d) 45^0 (Leading edge facing the cloud) (LEFC), (e) horizontal (Trailing edge facing the cloud) (TEFC), and (f) horizontal (Leading edge facing the cloud) (LEFC). The model used for the rotation mode is shown in Figure 17 (a). In the experimental configuration, compared to the simulation, the blade in the vertical position referred to as facing the cloud is pointing directly downwards towards the ground plane, where after the tip was pitched in steps of 45°. Also referred to as 45°, leading or Trailing edge facing the cloud.

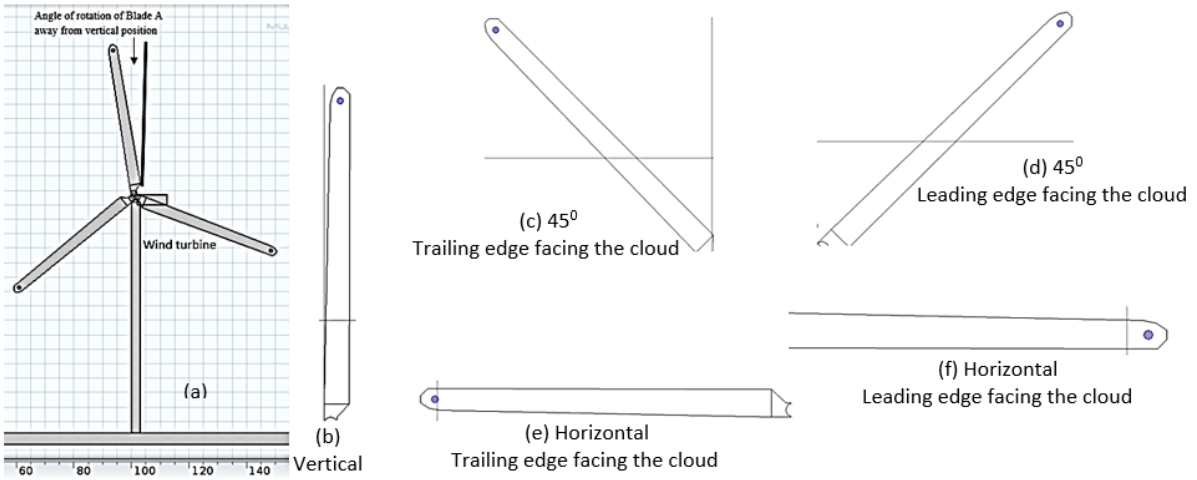

Figure 17: (a) Model for rotation mode, (b, c, d, e and f) Arrangement of blade sample

A 3m GFRP blade tip elevated above the ground electrode in a laboratory is shown Figure 18.

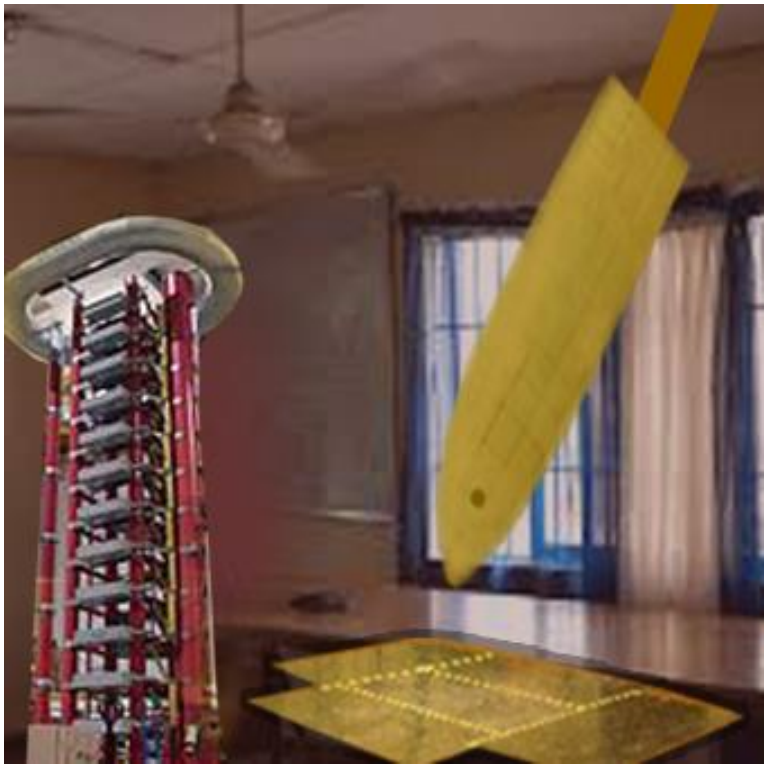

Figure 18: A 3m GFRP blade tip elevated above the ground electrode

Experimental conditions

The protected blade tip was tested and the test conducted according to IEC 61400-24. The experiments were performed with the model blade set as a high-voltage electrode. The receptor is a disk-type with a metal disk 10 mm diameter, it is covered with a flat metal braid set on the surface of the modal blade. The polarity of the applied voltage is positive and negative.

RESULTS AND DISCUSSION

An efficient receptor is one with highest number of discharge inception from the receptor and minimum at the tip, leading edge, trailing edges and the entire blade surface.

In evaluating the efficiency of receptor on discharge interception, the experiment is conducted on the wind turbine, first without receptor and then the blade is rotated. The polarity of the charge removed from the thundercloud can be used to sub-divide lightning into negative and positive flashes. A negative flash results in negative charge being transferred to the earth from the thundercloud. They are the dominant type of lightning flashes, around 90% of all cloud to ground, exhibiting the steepest current impulses (highest di/dt). A positive flash lowers positive charge from the thundercloud to the earth, around 10 % of all cloud to ground flashes, exhibiting the most powerful current parameters (higher I, Q and W/R).

The experimental results follow a regular pattern for both positive and negative polarity and are similar to that in literature, however, since negative flashes are the dominant type of lightning and are more pertinent to the present experiment, only results for negative polarity are presented.

Experiments with and without Receptor on the Model Blade

The test results are summarized as follows.

(1) Experiments without receptor on the model blade

Without the receptor, discharge to the model blade occurred at different points.

(2) Experiments with receptor on the model blade

The experimental results with various blade positions are shown in Table 6. The results are summarized as follows.

(1) For blade tip facing the ground (Also referred to as vertical position in Figure 17), whether polluted or unpolluted, 100% of the discharge initiated from the receptor.

(2) In the case of 45^0 (Trailing edge facing the cloud) (TEFC), 99% of the discharge initiated from the receptor, however, 1% of the discharge initiated from the blade trailing edge and was more for the polluted blade condition.

(3) In the case of 45^0 (Leading edge facing the cloud) (LEFC), the observation was similar to 2 above, 99% of the discharge initiated from the receptor, and 1% of the discharge initiated from the blade leading edge and was also more for the polluted blade condition.

(4) In the case of horizontal (Trailing edge facing the cloud) (TEFC), the observation was similar to 2 above.

(5) In the case of horizontal (Leading edge facing the cloud) (LEFC), the receptor performance at this position was relatively better, 100% of the discharge initiated from the receptor.

Other forms of discharge were also observed, puncture discharges from inside the blade sample to the ground occurred. In some cases, discharge incepted from a receptor progressed on the blade surface and then terminated to the ground.

Image of a negative discharge terminating on the ground is shown in Figure 19.

Figure 19: discharge from the blade tip towards the ground plane

Table 6: No of discharge initiation for a blade-to-ground gap

Blade tip angle from ground plane	Blade tip	Leading Edge	Trailing Edge	Receptor
-90^0	0	0	0	20
-45^0	0	1	0	19
0^0	0	0	0	20
45^0	0	0	1	19
90^0	0	0	1	19

Occasionally, discharge is initiated from the blade surface rather than the receptor, in this case, failure of receptor is discussed and determined. The points of discharge initiation correlated very well with experience with wind turbine blades in service that have been struck by lightning.

To pass the test by a receptor, all or majority of the discharge must initiate from the receptor. To fail, all or majority of the discharge have to initiate from the blade surface or other part of the wind turbine.

The maximum electric field strength on the model shown in Figure 14 with blade A at the vertical position is located between the receptor and the blade tip, which indicates that an upward leader will likely be initiated from that position. This agrees favourably well with the number of discharge initiation at this position in the experimental result indicating that the tip is worst hit. In addition, the figure reveals that the maximum electric field strengths locations are changing as the wind turbine is rotating. This is also in line with the number of discharge initiation and also corroborated result in (Abd-Elhady, Sabiha, & Izzularab, 2014), that the blade positions significantly affect the lightning attachment manner as well as the performance of the blade lightning protection systems. This result is also corroborated by the experimental result from the reduced size model in (Radicevic & Savic, 2011), that when the rotor of the reduced size wind turbine is rotating, a slight reduction in the number of direct strikes in the zone of the air-termination system on the blades was observed, as compared to the case when the rotor is stationary. Another very important correlation of the simulation with experimental result is that in most cases in the simulation, the maximum electric field strength locations on the trailing edge are higher than that of the leading edge which agrees with experimental result that the blade trailing edge attracts discharges more times than the blade leading edge. The implications of these two correlations are that as the blade is rotated, the points of leader inception changes and it is likely going to be more at the trailing edge than at the leading edge.

Obtained results of maximum electric field strength for both polluted and unpolluted blade conditions agree with the number of discharge initiation and upward leader initiation points in experimental results. It corroborated the experimental result in (Abd-Elhady, Sabiha, & Izzularab, 2014), that, in case of unpolluted surface, the air-termination system successfully captures surges more than in case of polluted surfaces. The level of damping on the polluted blade surface also supports the findings by Naka et al. (2006), that, regarding non-conductive blade, creeping discharge occurred more frequently in the polluted condition, and sometimes penetrative destruction was also observed.

CONCLUSION

The extended vertical tri-pole cloud charge distribution model for analysing lightning interactions with modern large wind turbines has been presented in this paper. The model is designed and analysed in Comsol Multiphysics and then evaluated with high voltage strike attachment test experiment. The vertical tri-pole cloud charge distribution model made from two positive charges and a negative charge representing the idealized gross charge structure of a thundercloud. The vertical tri-pole usually used to replicate the electric fields found under a thundercloud is extended to investigate the maximum electric field strength required for the initiation of upward leaders from wind turbines due to varying blade conditions. The model is intended for test on; various receptor sizes, discrete receptor position on the wind turbine, various lightning protection systems, effect of polluted blade surface, full scale blade length as well as scaled blade tip. As the blade rotates, it was tested in selected five positions to investigate the performance of wind turbine lightning protection systems on initiation of upward leader. The positions of the blade are chosen to determine the complete successes and failures of receptor. The proposed model has shown lightning discharges initiated from the

blade surface as well as the receptor, in this case, proficiency and failure of receptor is determined. To pass the test by a receptor, all or majority of the discharge must initiate from the receptor. To fail, all or majority of the discharge have to initiate from the blade surface or other part of the wind turbine. The simulation results are in agreement with that of the experiment and can be extended for larger wind turbines and for future work. The model can serve as a reliable test method in place of the EGM in IEC 61400 standard and can be implemented on impossible experiment for very large blades. Manufacturers may look at the finding of this work when dealing with the design aspects of very large future wind turbine.

REFERENCES

Abd-Elhady, A.M., Sabiha, N.A. & Izzularab, M.A. (2014). Experimental evaluation of air-termination systems for wind turbine blades. *Electric Power Systems Research, 107*, 133-143.

Alonso, M. & Irastorza, D. (2008). *Dynamic wind turbine lightning protection behaviour under strom conditions*. In 29th International Conference on Lightning Protection.

Ancona, D. & McVeigh, J. (2001). *Wind turbine-materials and manufacturing fact sheet.* Princeton Energy Resources International, LLC.

Bazelyan, E.M. & Raizer, Y.P. (2000). *Lightning physics and lightning protection*. CRC Press.

Cooray, V. (2010). *Lightning protection.* London: The Institution of Engineering and Technology.

Godson, I., et al. (2019). *Performance Enhancement of Lightning Protection Systems for Offshore Wind Turbine Blades*. In International Symposium on Lightning Protection (XV SIPDA), São Paulo, Brazil.

Imyanitov, I., Chubarina, E. & Shvarts, Y.M. (1971). *Cloud Electricity.* Gidrometeoizdat, Moscow.

Jeong-min, W., Sung-man, K. & Munno, J. (2024). *Analysis of polarity characteristics of lightning attachment and protection to wind turbine blades.* Elsevier.

MacGorman, D.R. & Rust, W.D. (1998). *The electrical nature of storms*. Oxford University Press on Demand.

Milelr, B. (2023). Vestas begins testing on first V164 80-metre blade. Retrieved from: http://www.windpoweroffshore.com/article/1211179/vestas-begins-testing-first-v164-80-metre-blade.

Minowa, M., et al. (2012). *A study of lightning protection for wind turbine blade by using creeping discharge characteristics*. In Lightning Protection (ICLP), 2012 International Conference. IEEE.

Montanyà, J., Van Der Velde, O., & Williams, E. R. (2014). Lightning discharges produced by wind turbines. *Journal of Geophysical Research: Atmospheres, 119*(3), 1455-1462.

Naka, T., et al. (2006). *Experimental studies on lightning protection design for wind turbine blades.* Proceedings of Euro-pean Wind Energy Association (EWEC), Athen, Greece.

Peesapati, V. & Cotton, I. (2009). *Lightning protection of wind turbines—A comparison of real lightning strike data and finite element lightning attachment analysis*. In Sustainable Power Generation and Supply. SUPERGEN'09. International Conference. IEEE.

Peesapati, V., Cotton, I., Sorensen, T., Krogh, T., & Kokkinos, N. (2011). Lightning protection of wind turbines–a comparison of measured data with required protection levels. *IET Renewable Power Generation*, *5*(1), 48-57.

Rachidi, F., Rubinstein, M., Montanya, J., Bermudez, J. L., Sola, R. R., Sola, G., & Korovkin, N. (2008). A review of current issues in lightning protection of new-

generation wind-turbine blades. *IEEE Transactions on Industrial Electronics*, *55*(6), 2489-2496.

Radičević, B. M., & Savić, M. S. (2011). Experimental research on the influence of wind turbine blade rotation on the characteristics of atmospheric discharges. *IEEE Transactions on Energy Conversion*, *26*(4), 1181-1190.

Rakov, V.A. & Uman, M.A. (2003). *Lightning: physics and effects*. Cambridge University Press.

Rodrigues, R., et al. (2009). Analysis of the thunderstorm activity in Portugal for its application in the lightning protection of wind turbines. *IEEE Latin America Transactions, 7*(5).

Sadiku, M.N. (2014). *Elements of electromagnetics*. Oxford University Press.

Shindo, T., Asakawa, A., & Miki, M. (2011). Characteristics of lightning strikes on wind turbine blades. Experimental study of the effects of receptor configuration and other parameters. *Electrical Engineering in Japan, 176*(3), 8-18.

Wang, D., et al. (2008). Observed characteristics of upward leaders that are initiated from a windmill and its lightning protection tower. *Geophysical Research Letters, 35*(2).

Warner, T. A., Lang, T. J., & Lyons, W. A. (2014). Synoptic scale outbreak of self-initiated upward lightning (SIUL) from tall structures during the central US blizzard of 1–2 February 2011. *Journal of Geophysical Research: Atmospheres*, *119*(15), 9530-9548.

Yoh, Y. & Shigeru, Y. (2011). *Proposal of lightning damage classification to wind turbine blades*. in *Lightning (APL),* 7th Asia-Pacific International Conference. IEEE.

Yokoyama, S. (2011). *Lightning protection of wind turbine generation systems*. in *Lightning (APL),* 7th Asia-Pacific International Conference. IEEE.

Zavareh, H.T. (2012). *Wind turbines protection against the lightning struck using a combined method*. In Renewable Energy and Distributed Generation (ICREDG), 2012 Second Iranian Conference. IEEE.

Zhou, H., et al. (2011). *Close electric field changes associated with upward-initiated lightning at the Gaisberg Tower*. In Lightning Protection (XI SIPDA), 2011 International Symposium. IEEE.

Zhou, H., Diendorfer, G., Thottappillil, R., Pichler, H., & Mair, M. (2012). Measured current and close electric field changes associated with the initiation of upward lightning from a tall tower. *Journal of Geophysical Research: Atmospheres*, *117*(D8).